The Cryosphere Discuss., 7, 2761–2800, 2013
www.the-cryosphere-discuss.net/7/2761/2013/
doi:10.5194/tcd-7-2761-2013

The Cryosphere Discussions
Open Access

Feedbacks and mechanisms affecting the global sensitivity of glaciers to climate change

B. Marzeion[1], **A. H. Jarosch**[2], **and J. M. Gregory**[3]

[1]Center of Climate and Cryopshere, Institute of Meteorology and Geophysics, University of Innsbruck, Austria
[2]Icelandic Meteorological Office, Reykjavík, Iceland
[3]NCAS-Climate, University of Reading, Reading, and Met Office Hadley Centre, Exeter, UK

Received: 31 May 2013 – Accepted: 4 June 2013 – Published: 17 June 2013

Correspondence to: B. Marzeion (ben.marzeion@uibk.ac.at)

Published by Copernicus Publications on behalf of the European Geosciences Union.

Abstract

Mass loss by glaciers has been an important contributor to sea level rise in the past and is projected to contribute a substantial fraction of total sea level rise during the 21st century. Here, we use a model of the world's glaciers in order to quantify equilibrium sensitivities of global glacier mass to climate change, and to investigate the role of changes in glacier hypsometry for long term mass changes. We find that 21st century glacier mass loss to a large degree is governed by the glaciers responding to 20th century climate change. This limits the influence of 21st century climate change on glacier mass loss, and explains why there are relatively small differences in glacier mass loss under greatly different scenarios of climate change. Because of the geographic distribution of glaciers, both temperature and precipitation anomalies experienced by glaciers are vastly stronger than on global average. The projected increase in precipitation partly compensates for the mass loss caused by warming, but this compensation is negligible at higher temperature anomalies since an increasing fraction of precipitation at the glacier sites it liquid. Loss of low-lying glacier area, and more importantly, eventual complete disappearance of glaciers, strongly limit the projected sea level contribution from glaciers in coming centuries. The adjustment of glacier hypsometry to changes in the forcing reduces the sensitivity of global glacier mass to changes in global mean temperature by a factor of two to three. This result is a second reason for the relatively weak dependence of glacier mass loss on future climate scenario, and helps explain why glacier mass loss in the first half of the 20th century was of the same order of magnitude as in the second half of the 20th century, even though the rate of warming was considerably smaller.

1 Introduction

Glaciers[1] have lost a substantial fraction of their mass during the past century (Cogley, 2009; Marzeion et al., 2012), with the globally averaged mass balance turning negative probably around 1850 (Leclercq et al., 2011). Within the 20th century, mass loss of glaciers was likely the largest single cause of sea level rise, followed by thermal expansion of the ocean, mass loss of the Greenland and Antarctic ice sheets, and changes in terrestrial water storage (Gregory et al., 2013). Even though the rise of global mean air temperature accelerated within the 20th century, the mass loss rate of glaciers during the second half of the 20th century was not higher than during the first half of the century (Leclercq et al., 2011; Marzeion et al., 2012).

Mass loss from glaciers will continue to contribute to sea level rise substantially during the 21st century, even though their total sea level rise potential is limited by their total mass, with the total ice mass in glaciers estimated as 35 ± 7 cm sea level equivalent (SLE, Grinsted, 2013), 43 ± 6 cm SLE (Huss and Farinotti, 2012), 41–52 cm SLE (depending on the assumed fraction of ice caps, Radić et al., 2013), or 49 ± 6 cm SLE (including the mass estimate for peripheral glaciers in Antarctica from Radić et al. (2013), Marzeion et al., 2012). Driven by climate scenarios obtained from the Coupled Model Intercomparison Project phase 5 (CMIP5) data base, and depending on the emission scenario applied (see van Vuuren et al., 2011, for an overview of the different representative concentration pathways, RCPs), the contribution of glaciers to sea level rise during the 21st century is estimated as 16 ± 4 cm SLE (RCP4.5) to 22 ± 4 (RCP8.5) by Radić et al. (2013), or as 15 ± 4 cm SLE (RCP2.6), 17 ± 4 cm SLE (RCP4.5), to

[1]Using the term *glaciers* we are referring to glaciers and ice caps excluding the Antarctic and Greenland ice sheets, but including the Antarctic and Greenland peripheral glaciers and ice caps.

22 ± 5 cm SLE (RCP8.5) by Marzeion et al. (2012)[2]. Remarkably, there is considerable overlap of the uncertainty ranges of projected mass loss from glaciers even for very different climate scenarios, for instance, RCP2.6 and RCP8.5, which during the period 2081–2100 arrive at a global mean temperature change of 1.2 ± 0.4 K and 3.8 ± 0.8 K respectively relative to 1986–2005. The overlap of uncertainty ranges in glacier projections for these scenarios is not caused by the uncertainties of the glacier models, but by the spread of the ensemble of climate projections used to drive the glacier models, which gives a spread in glacier mass loss projections that is relatively large compared to the ensemble mean, and because the rates of mass loss projected for the different RCP scenarios are relatively similar during the 21st century. The latter also reflects the observation that there was no simple relation between rates of glacier mass loss and temperature change during the 20th century.

There are a number of assessments that explain some of the mechanisms responsible for this behavior. E.g., Huss (2012) points out that in the Alps during the period 1900 to 2011, the mass balance year of 2003 had the most negative specific mass balances, but the greatest loss of ice volume occurred in 1947, when the glacier surface area was considerably larger. But it is not only changes in surface area that change a glacier's response to climate forcing over time: dynamic changes in ice thickness and terminus elevation, reflected together in changes of the ice surface topography, feed back to the mass balance and dampen (in case of terminus elevation) or enhance (in case of thickening/thinning) the glacier's response to climate forcing (Huss et al., 2012). Paul (2010) comes to the similar conclusion that without changes in glacier hypsometry, mass balances in the Alps since 1850 would have been two to three times as negative as they have actually been observed. This issue has also been discussed in detail by Leclercq et al. (2010) and Huss et al. (2010).

[2]Note that there are several more estimates of 21st century glacier mass loss based on climate scenarios obtained from the CMIP3 database, which are not mentioned here because of the limited comparability.

Since dynamic adjustments of a glacier's hypsometry to changed forcing conditions do not happen instantaneously, glaciers may be found out of balance with climate forcing long after a change in the climate forcing occurred. Jóhannesson et al. (1989) and Oerlemans (2001) developed different frameworks that allow the estimation of the response time of a glacier's hypsometry to changes in climate forcing.

But there are no studies that investigate how mass balances of glaciers are influenced by these mechanisms on a global scale, i.e. to what extent present and future sea level rise from glaciers reflects past climate change, and to what extent past and future sea level rise from glaciers is influenced by the feedback of glacier hypsometry changes on glacier mass balance. In order to illuminate these issues we use the global glacier model of Marzeion et al. (2012) which captures most – but not all – of the relevant mechanisms to study the glaciers' response to a number of idealized climate forcings. We briefly describe the glacier model in Sect. 2. We present experiments determining equilibrium sensitivities of the world's glaciers, including a distinction of the effects of changes in temperature and precipitation, in Sect. 3. The effect of glacier hypsometry changes on the response of glaciers to future climate change is investigated in Sect. 4 by keeping various aspects of glacier hypsometry fixed in the model. We discuss the results in Sect. 5 and conclude in Sect. 6.

2 Description of the glacier model

The glacier model is based on calculating the annual specific mass balance B for each of the world's individual glaciers as

$$B = \left[\sum_{i=1}^{12}\left[P_i^{\text{solid}} - \mu^* \cdot \max\left(T_i^{\text{terminus}} - T_{\text{melt}}, 0\right)\right]\right] - \beta^* \quad (1)$$

where P_i^{solid} is the area mean monthly solid precipitation onto the glacier surface, which depends on the monthly mean total precipitation and the temperature range between

TCD
7, 2761–2800, 2013

the glacier's terminus and highest elevations (i.e., temperature at terminus elevation below a certain threshold implies all precipitation is solid, temperature at the glacier's maximum elevation above the threshold implies all precipitation is liquid, and within that temperature range, the precipitation fraction is interpolated linearly, see Marzeion et al. (2012) for a detailed description), μ^* is the glacier's temperature sensitivity, T_i^{terminus} is the monthly mean air temperature at the location and elevation of the glacier's terminus, T_{melt} is the monthly mean air temperature above which ice melt is assumed to occur, and β^* is a bias correction. The model does not attempt to capture the full energy balance at the ice surface, but relies on air temperature as a proxy for the energy available for melt (Ohmura, 2001; Hock, 2003; Sicart et al., 2008). P_i^{solid} and T_i^{terminus} are determined based on gridded climate observations (New et al., 2002; Mitchell and Jones, 2005), to which temperature and precipitation anomaly fields from CMIP5 models are added, depending on the experiment performed (see descriptions of experimental setup in Sects. 3 and 4). Changes affecting the glacier hypsometry (i.e. changes in its volume, surface area, and elevation range) are reflected in the determination of P_i^{solid} and T_i^{terminus}, and are modeled based on B, and on linearly adjusting the glacier's surface area and length towards their respective values obtained from volume-area and volume-length scaling (Bahr et al., 1997; Bahr, 1997). I.e., the surface area change dA of a glacier during each mass balance year t is calculated as

$$\mathrm{d}A = \frac{1}{\tau_{\mathrm{A}}}\left(\left(\frac{V(t+1)}{c_{\mathrm{A}}}\right)^{1/\gamma} - A(t)\right) \tag{2}$$

where τ_{A} is the area relaxation time scale, $V(t+1)$ is the glacier's volume at the end of the mass balance year, c_{A} and γ are scaling parameters (Bahr et al., 1997; Bahr, 1997), and $A(t)$ is the surface area of the glacier at the end of the preceding mass balance year. Similarly, length changes dL (and terminus elevation changes associated with them through the glacier steepness) during each mass balance year are estimated as

$$dL = \frac{1}{\tau_L}\left(\left(\frac{V(t+1)}{c_L}\right)^{1/q} - L(t)\right) \tag{3}$$

where τ_L is the length relaxation time scale, c_L and q are scaling parameters (Bahr et al., 1997; Bahr, 1997), and $L(t)$ is the glacier's length at the start of the mass balance year. The glacier length response time scale τ_L is estimated roughly following Jóhannesson et al. (1989) as

$$\tau_L(t) = \frac{V(t)}{\sum_{i=1}^{12} P_{i,\mathrm{clim}}^{\mathrm{solid}}} \tag{4}$$

where $P_{i,\mathrm{clim}}^{\mathrm{solid}}$ is the monthly climatological solid precipitation onto the glacier surface. The glacier area response time scale is estimated as

$$\tau_A(t) = \tau_L(t)\frac{A(t)}{L(t)^2} \tag{5}$$

based on the assumption that area changes caused by glacier width changes occur instantaneously, while area changes caused by glacier length changes occur with the time scale of glacier length response.

The temperature sensitivity μ^* of a glacier is estimated by first determining a 31 yr reference period centered around the year t^* for each of the glaciers with available mass balance measurements in Cogley (2009). To determine this reference period, we first assume that the glacier in present day hypsometry is in equilibrium with a climatological forcing, i.e. that

$$B = \sum_{i=1}^{12}\left[P(t)_{i,\mathrm{clim}}^{\mathrm{solid}} - \mu(t)\cdot\left(\max\left(T(t)_{i,\mathrm{clim}}^{\mathrm{terminus}} - T_{\mathrm{melt}}, 0\right)\right)\right] = 0 \tag{6}$$

where $P(t)^{\text{solid}}_{i,\text{clim}}$ and $T(t)^{\text{terminus}}_{i,\text{clim}}$ are the monthly climatological values of P^{solid}_i and T^{terminus}_i, during the 31 year period centered around the year t. We obtain a total of 109 monthly climatologies of precipitation and temperature (the data set of Mitchell and Jones (2005) provides 109 years of monthly precipitation and temperature), and subsequently obtain an estimate of μ from Eq. (1) for each of the 109 choices of t. We then apply the glacier model to all glaciers for which direct mass balance observations are available, and for all values of μ. For each of these glaciers, we identify t^* as that year, for which applying the corresponding temperature sensitivity, denoted by μ^*, in the glacier model yields the smallest bias of modeled versus observed mass balances. This minimum bias is denoted by β^*.

For glaciers without observed mass balances (i.e., the vast majority of glaciers), t^* is interpolated from surrounding glaciers with mass balance observations, and μ^* is subsequently determined from applying Eq. (1) using precipitation and temperature obtained from the climatology centered around the year t^*, i.e.

$$\sum_{i=1}^{12}\left[P(t^*)^{\text{solid}}_{i,\text{clim}} - \mu^* \cdot \left(\max\left(T(t^*)^{\text{terminus}}_{i,\text{clim}} - T_{\text{melt}}, 0\right)\right)\right] = 0. \tag{7}$$

The bias correction β^* is determined by interpolating the minimized bias obtained during the determination of t^* from surrounding glaciers with mass balance observations. A cross validation of the determination of μ^* shows that the spatial interpolation of t^* leads to substantially smaller errors than the spatial interpolation of μ^* (Marzeion et al., 2012). This can be understood as an effect of neighboring glaciers experiencing a similar history of climate forcing, but having potentially very different temperature sensitivities.

Initial values for surface area and elevation distribution of a glacier are obtained by draping ice outlines from the Randolph Glacier Inventory (RGI, Arendt et al., 2012) version 1 over version 2 of the ASTER global digital elevation model (GDEM), applying a suitable watershed algorithm (Ehlschlaeger, 1989) to separate ice complexes into individual glaciers, and extracting glacier elevation statistics from the GDEM. The model accounts for the differing dates of surface area measurement in the RGI by ensuring that the observed glacier extent is reproduced in the year of observation. The initial volume at the start of the model run is determined from this constraint: iteratively, we determine the ice volume (as well as surface area, length and terminus elevation, following the scaling relations mentioned above) at the start of the simulation that yields the observed surface area in the year of observation. Unless mentioned otherwise, all the runs of the glacier model presented here were initialized using the "historical" experiment of the respective CMIP5 model.

A more detailed and complete description of the determination of the model's parameters, both glacier-specific and global, and a comprehensive validation of the model can be found in Marzeion et al. (2012). Uncertainties of the modeled results are obtained by propagating the uncertainties of the modeled specific mass balance, which are determined independently during a leave-one-glacier-out cross validation, through the entire model system, also taking into account uncertainties of the representation of the dynamic glacier response to volume changes. The propagated and temporally accumulated uncertainties themselves are also independently validated using geodetically measured volume and surface area changes (see Marzeion et al., 2012).

3 Equilibrium sensitivities

3.1 Experimental setup and forcing

Results from 15 different CMIP5 experiments (see Table 1) were used to force the glacier model in the equilibrium experiments. For each of the RCP8.5 experiments, monthly anomaly fields of precipitation and near surface air temperature were determined relative to the monthly climatology of 1961 to 1990. Then, monthly climatologies of the anomalies were determined for each overlapping 30 yr period contained in the combined historical and RCP8.5 experiment (i.e., between 1850 or 1860 and 2100 or

TCD
7, 2761–2800, 2013

2300, depending on the climate model, see Table 1). From this data set, the climatological anomaly fields of precipitation and temperature were extracted for global mean temperature anomalies of 1 to 10 K. (The number of fields extracted from each CMIP5 experiment therefore depends on the maximum global temperature anomaly reached over a 30 yr mean, and since the global mean temperature anomalies do not necessarily contain the required integer anomalies, we took the anomaly field with the smallest difference in global mean temperature anomaly. This difference is smaller than 0.1 K for all cases.) These anomaly fields were added to the observed climatological fields of New et al. (2002) to obtain the climate forcing for the glacier model. Additionally, the glacier model was forced by the observed climatological fields of New et al. (2002) only, i.e. without any modeled anomalies, giving a global mean anomaly of 0 K. To obtain the equilibrium response of the glaciers to this forcing, the same forcing was repeatedly applied for each glacier until volume changes of the glacier became negligible. This was defined to be the case when the volume change over the last 100 modeled years was smaller than 1 % of the glacier volume. Reaching the equilibrium took up to approximately 700 yr for some glaciers. On the global scale, ice volume changes are small after 200 years (Fig. 1). Note that in an experimental setup like this, glaciers may reach a true equilibrium, while the state of the climate system that was used to drive the glaciers into equilibrium is not itself an equilibrium.

Since both temperature and precipitation anomalies affect the mass balance of glaciers, in order to isolate the effects of both, the experiment was repeated once applying only the temperature anomaly fields, i.e. ignoring any precipitation anomalies resulting from future climate change, and once applying only the precipitation anomaly fields, i.e. ignoring the temperature anomalies.

TCD
7, 2761–2800, 2013

3.2 Results

Figure 2 shows the resulting equilibrium volume changes of the worlds glaciers as a function of global mean temperature anomaly[3]. When forced with the observed climatology of 1961 to 1990, glaciers would lose mass corresponding to 8.1 ± 0.3 cm sea level rise relative to the same time period, before reaching a new equilibrium (note that the uncertainty range given – one standard error – to a large degree depends on the time scale of glacier adjustment in this experimental setup, since errors are accumulated over time). The equilibrium sensitivity to small temperature and associated precipitation changes with respect to the climatology is of the order of 130 mm SLE K^{-1} (see Table 2) with considerable differences between different climate models. The sensitivity decreases to zero for progressively larger temperature changes, because of the reduction in the ice mass that remains to be removed.

Generally speaking, global mean precipitation increases with increasing global mean temperatures (e.g., Andrews et al., 2010). It can therefore be expected that the precipitation anomalies associated with the warming dampen the glacier equilibrium response to the warming. This is confirmed in Fig. 3, showing the additional equilibrium mass loss when precipitation anomalies from the climate model are not applied to the glacier model. Increasing precipitation decreases the glacier mass loss by the order of 15 mm SLE K^{-1} (see Table 2), again with considerable differences between the climate models. But for warming greater than 1 K this dampening effect of precipitation vanishes, even though precipitation can be expected to increase further. The reason is

[3]Peripheral glaciers in Antarctica cannot be modeled directly by our model because the climate data sets of New et al. (2002) and Mitchell and Jones (2005) do not cover Antarctica. Estimates for volume change of peripheral glaciers of Antarctica are therefore obtained by upscaling (which may be problematic since snow fall increase may dominate increased melt see, Barrand et al., 2013), and no estimate of the volume of Antarctic peripheral glaciers is obtained from the model. Therefore, the right axis of Fig. 2 (% volume loss) may exceed 100 %. See Marzeion et al. (2012) for a discussion of the implications of this approach to obtain results for peripheral Antarctic glaciers.

TCD
7, 2761–2800, 2013

that with higher temperatures an increasing fraction of precipitation is liquid and does not contribute to glacier mass gain. At very high temperature anomalies, essentially all precipitation falling at the glaciers becomes liquid, such that changes in the amount of precipitation do not effect glacier mass balance in our model.

It would therefore be wrong to assume that precipitation anomalies at the glacier sites are small – it is just that much of the increasing precipitation is liquid because of the increased temperatures: Fig. 4 shows the additional equilibrium mass loss of glaciers when temperature anomalies are ignored (i.e., negative values imply glacier mass gain relative to Fig. 2). If the warming is ignored, precipitation changes associated with 4 K global mean temperature change would roughly cancel the mass loss associated with the combined temperature and precipitation anomalies at the same global mean temperature change (~400 mm SLE). At lower global mean temperature anomalies, the combined temperature and precipitation signal is stronger, at higher global mean temperature anomalies, the signal of precipitation alone is stronger.

To understand this rather strong effect of precipitation changes, it is helpful to set the global mean changes of temperature and precipitation into relation with the changes experienced by glaciers. Figure 5a shows the glacier surface area weighted mean temperature change for each climate model as a function of global mean temperature change. While there are strong differences between climate models, all of them project greater than average warming at the glacier sites, particularly at low temperature changes. The mean amplification factor at small temperature changes is 1.8 (i.e. at a global mean temperature change of 2 K, glaciers experience a mean temperature change of 3.6 K). This temperature amplification is easily explained by the geographical distribution of glaciers, which all are situated on land, which on average experiences a greater warming than the global mean (e.g., Sutton et al., 2007), and a large fraction of glaciers is located at high northern latitudes, where warming is also greater than at lower latitudes (e.g., Manabe et al., 1991). Since this Arctic temperature amplification to a large degree is caused by sea ice-related albedo reduction (Screen and Simmonds, 2010), it is consistent that the amplification factor experienced by glaciers decreases for high global mean temperature changes, since sea ice cover lost at lower temperatures may no longer influence the local albedo.

Glaciers are projected to experience an even stronger amplification of precipitation (Fig. 5b). The spread between the different climate models is even larger than for temperature, and the amplification is nearly independent of temperature. The positive correlation between temperature and precipitation anomalies is determined by the energy balance of the troposphere (Andrews et al., 2010).

4 Feedbacks of glacier hypsometry and mass balance

4.1 Experimental setup and forcing

All the projections of global glacier mass change during the 21st to 23rd centuries presented in (Marzeion et al., 2012) were repeated,

- once ignoring all the effects of glacier mass loss or gain on glacier hypsometry, i.e. glacier surface area and elevation distribution were held constant in time, as obtained from the RGI and GDEM, and glacier volume was treated as infinite, allowing the glacier to respond to changed climate forcing independent of the history of climate forcing.

- once including all the effects of glacier mass loss or gain on glacier hypsometry except for the terminus elevation, which was held constant in time, as obtained from the RGI and GDEM (i.e., surface area and volume evolving with time).

- once including all the effects of glacier mass loss or gain on glacier hypsometry except for the surface area, which was held constant in time, as obtained from the RGI (i.e., terminus elevation and volume evolving with time).

- once only including only the effect of mass loss on glacier volume, keeping surface area and elevation distribution constant in time, as obtained from the RGI and GDEM (i.e., only volume evolving with time).

The results of these experiments were then compared to the results of Marzeion et al. (2012) in order to isolate and quantify the feedbacks of different aspects of glacier hypsometry change with mass balance.

4.2 Results

4.2.1 Constant hypsometry, infinite ice volume

If all aspects of a glacier's hypsometry are held constant in time, and ice volume is treated as infinite, the glacier is prevented from approaching an equilibrium with climate forcing, and subjecting the glacier to climate change essentially becomes equivalent to transplanting a glacier into a future climate, without taking into account the temporal evolution of climate and glacier change that lead there. In this scenario, rates of glacier mass loss are easier to understand than accumulated mass loss, and shown in Fig. 6 as a function of global mean temperature, and as a function of glacier surface area weighted mean temperature. Independent of the applied scenario and climate model, rates of mass loss increase (for positive temperature anomalies) or decrease (for negative temperature anomalies) roughly quadratical with temperature. A quadratic relation can be expected from Eq. (1), where both solid fraction of precipitation and monthly ablation, and length of the seasons are related almost linearly to temperature (for length of seasons and solid fraction of precipitation this is only true within certain bounds). We therefore fitted a quadratic function for all scenarios and all models, once using the global mean, and once using glacier surface area weighted temperature anomaly.

Table 3 summarizes the parameters of the function, and the mean goodness-of-fit (measured by the root mean square error, RMSE, of the fitted curve). We find a contribution of roughly 1 mm SLE yr^{-1} mass loss that corresponds to the adjustment of glaciers to past climate change, discussed Sect. 3, and is therefore independent of temperature anomalies. This contribution implies substantial future glacier mass loss even without further warming. The magnitude here however is substantially higher than the magnitude of the mass loss rates found in the equilibrium experiments (the line corresponding to "CRU" in Fig. 1, of the order of 0.5 mm SLE yr^{-1} at the start of the experiment), indicating that glacier hypsometry changes dampen the glaciers response to climate change.

A further contribution is linearly related to temperature anomalies, and of the order of 0.75 mm SLE yr^{-1} K^{-1} if glacier surface area weighted temperature anomaly is used, and of the order of 1.5 mm SLE yr^{-1} K^{-1} if global mean temperature anomaly is used. This contribution corresponds to the changes in solid precipitation and ablation, and the decreased sensitivity of glacier surface area weighted temperature anomaly is consistent with the temperature amplification experienced by the glaciers (Fig. 5). Finally, a quadratic contribution of roughly 0.22 mm SLE yr^{-1} K^{-2} (glacier surface area weighted temperature) or 0.73 mm SLE yr^{-1} K^{-2} (global mean temperature) is related to the interaction of changes in the length of seasons and changed temperature and solid precipitation.

Based on a linear approximation (i.e., ignoring the quadratic contribution), Gregory and Oerlemans (1998) estimate the linear sensitivity to 0.30 ± 0.15 mm SLE yr^{-1} K^{-1}, and Meehl et al. (2007) estimate it to 0.80 ± 0.33 mm SLE yr^{-1} K^{-1} based on observations, and to 0.61 ± 0.12 or 0.49 ± 0.13 mm SLE yr^{-1} K^{-1} based on different models (all using global mean temperature). To better understand our strongly enhanced sensitivity, we estimated a linear sensitivity for the case of fixed glacier hypsometry as before, but this time driving the glacier model with past, observed climate variability (Mitchell and Jones, 2005), essentially reproducing the method applied by Meehl et al. (2007) in our model. This experiment results in a linear sensitivity of 0.50 ± 0.59 mm SLE yr^{-1} K^{-1}, consistent with all the previous results (the error range given is the 95 % confidence interval, and is large because of a relatively weak correlation of mass loss rates with global mean temperature anomalies). This indicates that the reason for the substantially different sensitivities when determined based on either future or past climate change is that the present glacier hypsometries have already responded to past climate change. I.e., the actual sensitivity for a fixed reference hypsometry is high, but the sensitivity is strongly dampened by the glaciers' hypsometry response. This response has already had a considerable influence on past glacier mass change.

If the mean of the parameters across the different climate models is applied, the fit of the curve based on the glacier surface area weighted temperature anomaly is substantially better than the fit based on the global mean temperature anomaly (RMSE about half as big, Table 3). This indicates that differences in the spatial patterns of the temperature anomaly are responsible for a considerable fraction of the different responses of global glacier mass to climate change. Differences in precipitation anomaly patterns, and history of the climate forcing, must be responsible for the rest.

The temporally accumulated mass loss from the experiment with constant hypsometry and infinite volume is shown in Fig. 7. From this too it is apparent that changes in glacier hypsometry and volume must impose strong limits on glacier mass loss in reality, since the projected sea level rise far exceeds the (fixed) initial ice volume. Given the excessive projected mass loss of this experiment, it is clear that the ice mass must be the dominant limiting factor of future mass loss in all the scenarios, and for all climate models.

Plotting the temporally integrated glacier mass loss of this experiment as a function of the temporally integrated mass loss of Marzeion et al. (2012, see Fig. 8), it becomes apparent that glacier hypsometry and volume changes dampen the mass loss response of glaciers to climate change even for fairly small mass losses of less than 10 mm SLE, supporting the conclusion that the feedbacks considered here have already played a role in shaping the 20th century mass response of glaciers to climate change.

4.2.2 Constant terminus elevation

Changes in glacier terminus elevation can be expected to provide a negative feedback to the glacier mass balance, since a glacier losing mass eventually retreats to higher elevation, where colder temperatures prevail. Without the possibility of a response of the glacier terminus to mass balance anomalies, glaciers cannot reach an equilibrium with a changed climate, as in the approach taken e.g. by van de Wal and Wild (2001) and Slangen and van de Wal (2011). Figure 9 shows that if this feedback is ignored, glaciers would lose substantially more mass under global warming. Figure 10 shows that the mass loss is not only greater under all scenarios, but also at all times the rates of mass loss are higher. The feedback is strongest in the RCP2.6 scenario, and weakest in the RCP8.5 scenario. The reason for this difference is the availability of glaciers that may be affected: in the RCP2.6 scenario, mass loss is relatively small and relatively few glaciers disappear completely, implying that many glaciers are affected by the feedback. But under a scenario of greater warming, many glaciers lose all their mass, implying that terminus elevation does not matter any longer for their mass balance. Figure 11, showing the difference in mass loss in 2300, i.e. at a time when the fully responsive model is close to equilibrium, confirms that the effect of changing terminus elevations is largely a function of past mass loss, independent of climate model and RCP scenario. During the transient period, the relation between mass past mass loss and the terminus elevation feedback is more complex, since terminus elevation changes lag behind glacier mass changes, with lag times being different for each glacier due to the different response time scales.

4.2.3 Constant surface area

In the warming climate of the RCP scenarios, specific mass balances are mostly negative, and glacier surface areas are generally shrinking. Keeping the surface area of the glaciers constant, i.e. applying the negative specific mass balances over a too great area, should presumably lead to a faster mass loss of glaciers. Figures 9 and 10 shows that this is the case only for a short period of a few decades, and only to a very small extent.

Generally speaking, keeping surface area constant leads to weaker glacier mass loss, with stronger weakening for warmer scenarios. The mechanism explaining this behavior is based on an asymmetric effect of climate variability on mass balances: if a glacier loses all its mass but the surface area is held constant, a negative mass balance will not produce any mass loss. But a positive mass balance, that may and will occur because of climate variability, will lead to (at least temporary) storage of mass in the glacier – until it is lost again during the following year(s). The more glaciers have lost all mass, the more glaciers will be influenced by this asymmetry, explaining why this effect gets stronger with increasing global mass loss (confirmed in Fig. 11). In the case considered here, where surface area is held constant, but the terminus is allowed to retreat to higher elevations, this effect is particularly pronounced, since it leads to increasing accumulation areas of the glaciers. Thus, the apparently reduced glacier mass loss assuming constant area arises because snow occasionally survives the summer within the assumed area, and is counted as part of the glacier mass, even though the glacier has contracted. By contrast, in the reference experiment with evolving hypsometry, the area under consideration contracts with th e glacier, and these temporary snowfields are not counted.

This way of counting sporadic snow as glacier ice should therefore not lead to the conclusion that surface area change provides a positive feedback to the mass balance – but it raises the question of how long a snow field has to exist before it will be counted as a glacier. Concerning the climate of the next few centuries this problem is probably not relevant, since it is hard to imagine a situation in which glaciers would start to grow, or new glaciers would come into existence. But it illustrates the conceptual problem of applying a glacier model of this type – i.e. relying on pre-defined glacier entities – in a climate susceptible to glacier growth.

TCD
7, 2761–2800, 2013

4.2.4 Constant terminus elevation and surface area

The scenario of constant area is not particularly relevant for understanding how glaciers behave, but it helps us to understand the combined effect of keeping both surface area and terminus elevation constant. This turns out to be very close to a simple linear superposition of keeping either terminus position or surface area separately constant. For small mass losses, the terminus elevation feedback prevails, and mass loss is accelerated, while for great mass losses, the surface area effect prevails, and mass loss is decelerated (Figs. 9, 10 and 11).

5 Discussion

In the global view, glaciers are considerably out of balance with the climate of the recent past, and glacier mass loss would continue even if climate would no longer change. Using observed accumulation-area ratios, Mernild et al. (2013) come to the conclusion that glaciers are already committed to a mass loss of 163 ± 73 mm SLE. While this estimate is higher than ours, a direct comparison with our results is not possible because of different reference times. But considering that they included observations up to 2010, whereas our reference period is 1961–1990, our estimate is probably consistent with theirs. Glacier mass loss during the next decades is therefore to a large extent predetermined from the past. This helps explain why there is great similarity in glaciers response to widely differing climate scenarios (Marzeion et al., 2012; Radić et al., 2013). Our result that the wide ensemble spread within each RCP scenario to a large extent is attributable to differences in temperature anomaly patterns is in line with the results of Giesen and Oerlemans (2013), even though not directly comparable since their model involves – apart from precipitation – atmospheric transmissivity as a forcing parameter. Giesen and Oerlemans (2013) also report that applying changes in temperature only increased the glaciers response to future warming significantly, but the compensation by increasing precipitation in our case is not as strong as in theirs.

Observed sea level rise during the 20th century can only be explained if the glaciers' contribution did not develop in parallel to global mean temperature, but was high already in the first half of the 20th century (Gregory et al., 2013). Our result that changes in glacier hypsometry play a significant role in shaping the glaciers' response to climate change, in particular that loss of low-lying surface area (i.e., terminus retreat to higher elevations) decreases the sensitivity is critical for explaining the strong glacier mass losses during the first half of the 20th century. Being able to explain, and account for this mechanism is also important for the ability of process based projections of sea level rise (Church et al., 2013). Knowledge of the equilibrium response of glaciers to climate change is furthermore necessary in order to develop scenarios of long-term sea level rise (Levermann et al., 2013).

By providing a positive feedback on the mass balance, ice thickness changes may be more important than terminus retreat in determining the mass balance response to climate change for some glaciers (Raymond et al., 2005). Particularly if the response of the glaciers is not dynamic, i.e. ice is melting over a large fraction, or all of the surface, ice thickness change may become important (Paul and Haeberli, 2008). Similarly, for glaciers with long, flat tongues, even a dynamic response to volume change may not necessarily lead to strong changes in terminus elevation, but the surface topography may still change considerably (Larsen et al., 2007; Bolch et al., 2008). The glacier model does not explicitly account for ice thickness change and associated changes in the surface topography that are unrelated to surface area change and terminus elevation. It is therefore not possible to isolate this effect here. However, we argue that while ice thickness change is not considered explicitly, it is contained in the model implicitly – more specifically, in the glaciers' temperature sensitivity μ^*: the ice thickness-mass balance feedback increases a glacier's sensitivity to temperature change, by amplifying the temperature anomalies at the ice surface. Since μ^* is essentially calibrated by determining a value that results in the best fit to observations (which of course include the feedback), and since the cross validation of the model in Marzeion et al. (2012) does not indicate a significant bias of modeled mass balances, independent of the length of the observation time series, we can conclude that the omission of explicitly including ice thickness changes in the model does not affect the reliability of the model's results. It would be feasible to explicitly include this mechanism, and it seems desirable to do so in order to be able to quantify it globally. We deliberately chose not to do this here, since it would require a complete recalibration of the model, which would inhibit the direct comparison with the results of (Marzeion et al., 2012). Moreover, the results of Paul (2010) and Huss et al. (2012) indicate that the combined effect of glacier surface topography changes is dampening the glaciers' response to climate forcing over long timescales, even though this may be arguably different for individual glaciers (Harrison et al., 2009). The increase of the sensitivity by a factor of two to three if glacier hypsometry is held constant reported by Paul (2010) for the European Alps is consistent with our results for the global scale.

Other potentially important feedbacks not included in the model but meriting thorough evaluation include e.g. changes of ice albedo due to accumulation of dust on melting glaciers (Oerlemans et al., 2009), and changes to the longwave radiation energy budget from newly exposed rock faces surrounding the glacier.

6 Conclusions

We have used a model of glacier response to climate change to quantify the equilibrium sensitivity of the global ice mass in glaciers, and to distinguish the respective contributions of temperature and precipitation anomalies. Because of the geographic distribution of glaciers, the temperature and precipitation change experienced by glaciers is far greater than the global mean. Precipitation anomalies projected for the future dampen the mass loss of glaciers, but their effect is strongly limited by the increasing temperatures, which increases the liquid fraction of precipitation on the glaciers.

We find that glacier mass loss during the 21st century is to a significant degree a response to 20th century climate change. This partly explains the relatively weak dependence of 21st century mass loss on future greenhouse gas emissions. A second reason is that the loss of glacier mass imposes a strong restriction to the rate of loss for a given climate. Results from methods not accounting for finiteness of ice mass available for melting, e.g. by extrapolating current rates of mass loss, or even increases of rates of mass loss (Meier et al., 2007), will therefore yield substantial overestimates.

Thirdly, changes of glacier hypsometry reduce the response of glaciers to warming, and need to be considered in explaining the observed rates of mass loss during the 20th century and the projected rates for the 21st century. Figure 9 summarizes our quantification of these effects, showing the dependence of the projected mass loss of glaciers during the next three centuries on how glacier hypsometry changes are represented in the model. The apparent positive feedback of shrinking glacier surface area on the glacier mass loss results from including sporadic snow in the glacier ice mass. The retreat of glacier termini to higher altitude also gives an important negative feedback.

Acknowledgements. This work was funded by the Austrian Science Fund (FWF): P22443-N21 and PP25362-N26, and supported by the Austrian Ministry of Science BMWF as part of the UniInfrastrukturprogramm of the Research Platform Scientific Computing at the University of Innsbruck.

References

Andrews, T., Forster, P. M., Boucher, O., Bellouin, N., and Jones, A.: Precipitation, radiative forcing and global temperature change, Geophys. Res. Lett., 37, L14701, doi:10.1029/2010GL043991, 2010. 2771, 2773

Arendt, A., Bolch, T., Cogley, G., Gardner, A., Hagen, J. O., Hock, R., Kaser, G., Paul, F., Radic, V., Bliss, A., Fountain, A., Mercer, A., Negrete, A., Giffen, B., Menounos, B., Kienholz, C., Mayer, C., Nuth, C., Burgess, D., Hall, D., Kriegel, D., Berthier, E., Burgess, E., Cawkwell, F., Wyatt, F., Hartmann, G., Wolken, G., Frey, H., Brown, I., Howat, I., Lund, J., Rich, J., Filbert, K., Andreassen, L., Copland, L., Beedle, M., Koenig, M., Sharp, M., Moelg, N., Sigurdsson, O., Rastner, P., Forester, R., LeBris, R., Pettersson, R., Wheate, R., Herreid, S., Vorogushin, S., Winsvold, S., Chinn, T., Hagg, W., and Manley, W.: Randolph

TCD
7, 2761–2800, 2013

Glacier Inventory 1.0: A Dataset of Global Glacier Outlines, Global Land Ice Measurements from Space, Boulder Colorado, USA, Digital Media, 2012. 2768

Bahr, D.: Global distributions of glacier properties: a stochastic scaling paradigm, Water Resour. Res., 33, 1669–1679, 1997. 2766, 2767

Bahr, D., Meier, M., and Peckham, S.: The physical basis of glacier volume-area scaling, J. Geophys. Res., 102, 355–362, 1997. 2766, 2767

Barrand, N., Hindmarsh, R., Arthern, R., Williams, C. R., Mouginot, J., Scheuchl, B., Rignot, E., Ligtenberg, S., van den Broeke, M., Edwards, T., Cook, A. J., and Simonsen, S. B.: Computing the volume response of the Antarctic Peninsula ice sheet to warming scenarios to 2200, J. Glaciol., 59, 397–409, 2013. 2771

Bolch, T., Buchroithner, M., Pieczonka, T., and Kunert, A.: Planimetric and volumetric glacier changes in the Khumbu Himal, Nepal, since 1962 using Corona, Landsat TM and ASTER data, J. Glaciol., 54, 592–600, 2008. 2780

Church, J. A., Monselesan, D., Gregory, J. M., and Marzeion, B.: Evaluating the ability of process based models to project sea-level change, Environ. Res. Lett., 8, 014051, doi:10.1088/1748-9326/8/1/014051, 2013. 2780

Cogley, J. G.: Geodetic and direct mass-balance measurements: comparison and joint analysis, Ann. Glaciol., 50, 96–100, doi:10.3189/172756409787769744, 2009. 2763, 2767

Ehlschlaeger, C.: Using the A^T search algorithm to develop hydrologic models from digital elevation data, in: International Geographic Information Systems (IGIS) Symposium, vol. 89, 275–281, 1989. 2768

Giesen, R. H. and Oerlemans, J.: Climate-model induced differences in the 21st century global and regional glacier contributions to sea-level rise, Climate Dynamics, doi:10.1007/s00382-013-1743-7, 2013. 2779

Gregory, J. M. and Oerlemans, J.: Simulated future sea-level rise due to glacier melt based on regionally and seasonally resolved temperature changes, Nature, 391, 474–476, 1998. 2775

Gregory, J. M., Church, J. A., White, N. J., Bierkens, M. F. P., Box, J. E., van den Broeke, M. G. C. J., Fettweis, X., Hanna, E., Leclercq, P. W., Marzeion, B., Oerlemans, J., Wada, Y., Wake, L. M., and van de Wal, R. S. W.: Twentieth-century global-mean sea-level rise: is the whole greater than the sum of the parts?, J. Climate, doi:10.1175/JCLI-D-12-00319.1, in press, 2013. 2763, 2780

Grinsted, A.: An estimate of global glacier volume, The Cryosphere, 7, 141–151, doi:10.5194/tc-7-141-2013, 2013. 2763

Harrison, W. D., Cox, L. H., Hock, R., March, R. S., and Pettit, E. C.: Implications for the dynamic health of a glacier from comparison of conventional and reference-surface balances, Ann. Glaciol., 50, 25–30, 2009. 2781

Hock, R.: Temperature index melt modelling in mountain areas, J. Hydrol., 282, 104–115, doi:10.1016/S0022-1694(03)00257-9, 2003. 2766

Huss, M.: Extrapolating glacier mass balance to the mountain-range scale: the European Alps 1900–2100, The Cryosphere, 6, 713–727, doi:10.5194/tc-6-713-2012, 2012. 2764

Huss, M. and Farinotti, D.: Distributed ice thickness and volume of all glaciers around the globe, J. Geophys. Res., 117, F04010, doi:10.1029/2012JF002523, 2012. 2763

Huss, M., Hock, R., Bauder, A., and Funk, M.: Reply to the Comment of Leclercq et al. on "100-year mass changes in the Swiss Alps linked to the Atlantic Multidecadal Oscillation", The Cryosphere Discuss., 4, 2587–2592, doi:10.5194/tcd-4-2587-2010, 2010. 2764

Huss, M., Hock, R., Bauder, A., and Funk, M.: Conventional versus reference-surface mass balance, J. Glaciol., 58, 278–286, 2012. 2764, 2781

Jóhannesson, T., Raymond, C., and Waddington, E.: Time-scale for adjustment of glaciers to changes in mass balance, J. Glaciol., 35, 355–369, 1989. 2765, 2767

Larsen, C. F., Motyka, R. J., Arendt, A. A., Echelmeyer, K. A., and Geissler, P. E.: Glacier changes in southeast Alaska and northwest British Columbia and contribution to sea level rise, J. Geophys. Res., 112, F01007, doi:10.1029/2006JF000586, 2007. 2780

Leclercq, P. W., van de Wal, R. S. W., and Oerlemans, J.: Comment on "100-year mass changes in the Swiss Alps linked to the Atlantic Multidecadal Oscillation" by Matthias Huss et al. (2010), The Cryosphere Discuss., 4, 2475–2481, doi:10.5194/tcd-4-2475-2010, 2010. 2764

Leclercq, P. W., Oerlemans, J., and Cogley, J. G.: Estimating the Glacier Contribution to Sea-Level Rise for the Period 1800–2005, Surv. Geophys., 32, 519–535, 2011. 2763

Levermann, A., Clark, P. U., Marzeion, B., Milne, G., Pollard, D., Radić, V., and Robinson, A.: The multi-millennial sea-level commitment of global warming, PNAS, accepted, 2013. 2780

Manabe, S., Stouffer, R., Spelman, M., and Bryan, K.: Transient responses of a coupled ocean-atmosphere model to gradual changes of atmospheric CO_2, Part I: annual mean response, J. Climate, 4, 785–818, 1991. 2772

Marzeion, B., Jarosch, A. H., and Hofer, M.: Past and future sea-level change from the surface mass balance of glaciers, The Cryosphere, 6, 1295–1322, doi:10.5194/tc-6-1295-2012, 2012. 2763, 2764, 2765, 2766, 2768, 2769, 2771, 2773, 2774, 2776, 2779, 2780, 2781, 2797, 2798, 2799, 2800

Meehl, G. A., Stocker, T. F., Collins, W. D., Friedlingstein, P., Gaye, A. T., Gregory, J. M., Kitoh, A., Knutti, R., Murphy, J. M., Noda, A., Raper, S. C. B., Watterson, I. G., Weaver, A. J., Zhao, Z.-C., et al.: Global climate projections, in: Climate Change 2007: The Physical Science Basis. Contribution of Working Group I to the Fourth Assessment Report of the Intergovernmental Panel on Climate Change, edited by: Solomon, S., Qin, D., Manning, M., Chen, Z., Marquis, M., Averyt, K. B. M. T., and Miller, H. L., Cambridge University Press, Cambridge, UK and New York, NY, USA, 2007. 2775

Meier, M. F., Dyurgerov, M. B., Rick, U. K., O'Neel, S., Pfeffer, W. T., Anderson, R. S., Anderson, S. P., and Glazovsky, A. F.: Glaciers dominate eustatic sea-level rise in the 21st century, Science, 317, 1064–1067, doi:10.1126/science.1143906, 2007. 2782

Mernild, S. H., Lipscomb, W. H., Bahr, D. B., Radić, V., and Zemp, M.: Global glacier retreat: a revised assessment of committed mass losses and sampling uncertainties, The Cryosphere Discuss., 7, 1987–2005, doi:10.5194/tcd-7-1987-2013, 2013. 2779

Mitchell, T. D. and Jones, P. D.: An improved method of constructing a database of monthly climate observations and associated high-resolution grids, Int. J. Climatol., 25, 693–712, doi:10.1002/joc.1181, 2005. 2766, 2768, 2771, 2775

New, M., Lister, D., Hulme, M., and Makin, I.: A high-resolution data set of surface climate over global land areas, Clim. Res., 21, 1–25, 2002. 2766, 2770, 2771

Oerlemans, J.: Glaciers and Climate Change, A. A. Balkema Publishers, Lisse, Abingdon, Exton, Tokyo, 2001. 2765

Oerlemans, J., Giesen, R., and Van Den Broeke, M.: Retreating alpine glaciers: increased melt rates due to accumulation of dust (Vadret da Morteratsch, Switzerland), J. Glaciol., 55, 729–736, 2009. 2781

Ohmura, A.: Physical basis for the temperature-based melt-index method, J. Appl. Meteorol., 40, 753–761, 2001. 2766

Paul, F.: The influence of changes in glacier extent and surface elevation on modeled mass balance, The Cryosphere, 4, 569–581, doi:10.5194/tc-4-569-2010, 2010. 2764, 2781

Paul, F. and Haeberli, W.: Spatial variability of glacier elevation changes in the Swiss Alps obtained from two digital elevation models, Geophys. Res. Lett., 35, L21502, doi:10.1029/2008GL034718, 2008. 2780

Radić, V., Bliss, A., Beedlow, A. C., Hock, R., Miles, E., and Cogley, J. G.: Regional and global projections of 21st century glacier mass changes in response to climate scenarios from

global climate models, Climate Dynamics, doi:10.1007/s00382-013-1719-7, 2013. 2763, 2779
Raymond, C., Neumann, T. A., Rignot, E., Echelmeyer, K., Rivera, A., and Casassa, G.: Retreat of Glaciar Tyndall, Patagonia, over the last half-century, J. Glaciol., 51, 239–247, 2005. 2780
Screen, J. A. and Simmonds, I.: The central role of diminishing sea ice in recent Arctic temperature amplification, Nature, 464, 1334–1337, 2010. 2772
Sicart, J., Hock, R., and Six, D.: Glacier melt, air temperature, and energy balance in different climates: The Bolivian Tropics, the French Alps, and northern Sweden, J. Geophys. Res., 113, D24113, doi:10.1029/2008JD010406, 2008. 2766
Slangen, A. B. A. and van de Wal, R. S. W.: An assessment of uncertainties in using volume-area modelling for computing the twenty-first century glacier contribution to sea-level change, The Cryosphere, 5, 673–686, doi:10.5194/tc-5-673-2011, 2011. 2777
Sutton, R. T., Dong, B., and Gregory, J. M.: Land/sea warming ratio in response to climate change: IPCC AR4 model results and comparison with observations, Geophys. Res. Lett., 34, L02701, doi:10.1029/2006GL028164, 2007. 2772
van de Wal, R. and Wild, M.: Modelling the response of glaciers to climate change by applying volume-area scaling in combination with a high resolution, GCM, 18, 359–366, 2001. 2777
van Vuuren, D., Edmonds, J., Kainuma, M., Riahi, K., Thomson, A., Hibbard, K., Hurtt, G., Kram, T., Krey, V., Lamarque, J., Masui, T., Meinshausen, M., Nakicenovic, N., Smith, S. J., and Rose, S. K.: The representative concentration pathways: an overview, Climatic Change, 109, 5–31, 2011. 2763

TCD
7, 2761–2800, 2013

Title Page
Abstract Introduction
Conclusions References
Tables Figures
◂ ▸
Back Close
Full Screen / Esc
Printer-friendly Version
Interactive Discussion

Table 1. CMIP5 models and experiments used for forcing.

Models	Historical	RCP2.6	RCP4.5	RCP6.0	RCP8.5
bcc-csm1-1	1850–2005	2006–2300	2006–2300	2006–2100	2006–2300
CanESM2	1850–2005	2006–2300	2006–2300	–	2006–2100
CCSM4	1850–2005	2006–2100	2006–2100	2006–2100	2006–2100
CNRM-CM5	1850–2005	2006–2100	2006–2300	–	2006–2300
CSIRO-Mk3-6-0	1850–2005	2006–2100	2006–2300	2006–2100	2006–2300
GFDL-CM3	1860–2005	2006–2100	2006–2100	2006–2100	2006–2100
GISS-E2-R	1850–2005	–	2006–2300	2006–2100	2006–2300
HadGEM2-ES	1860–2005	2006–2300	2006–2300	2006–2099	2006–2300
inmcm4	1850–2005	–	2006–2100	–	2006–2100
IPSL-CM5A-LR	1850–2005	2006–2300	2006–2300	2006–2100	2006–2300
MIROC5	1850–2005	2006–2100	1850–2100	2006–2100	2006–2100
MIROC-ESM	1850–2005	2006–2100	2006–2100	2006–2100	2006–2100
MPI-ESM-LR	1850–2005	2006–2300	2006–2300	–	2006–2300
MRI-CGCM3	1850–2005	2006–2100	2006–2100	2006–2100	2006–2100
NorESM1-M	1850–2005	2006–2100	2006–2300	2006–2100	2006–2100

Table 2. Equilibrium sensitivities obtained as the difference between the equilibrium states at global mean $\Delta T = 0$ K and global mean $\Delta T = 1$ K, and the anomalies of these sensitivities when either precipitation or temperature anomalies are ignored.

model	equilibrium sensitivity [$\mathrm{mm\,SLE\,K^{-1}}$]	Δ (equi. sensitivity) [$\mathrm{mm\,SLE\,K^{-1}}$] at P = const.	Δ(equi. sensitivity) [$\mathrm{mm\,SLE\,K^{-1}}$] at T = const.
bcc-csm1-1	139.1 ± 3.8	19.1 ± 5.3	-161.4 ± 5.4
CanESM2	135.1 ± 3.7	15.3 ± 5.3	-154.9 ± 5.4
CCSM4	154.8 ± 3.7	12.4 ± 5.3	-167.0 ± 5.3
CNRM-CM5	119.1 ± 3.8	18.0 ± 5.4	-153.2 ± 5.3
CSIRO-Mk3-6-0	91.6 ± 3.8	13.3 ± 5.3	-104.8 ± 5.3
GFDL-CM3	149.5 ± 3.7	16.3 ± 5.3	-165.6 ± 5.3
GISS-E2-R	128.9 ± 3.7	16.0 ± 5.3	-147.4 ± 5.3
HadGEM2-ES	156.3 ± 3.8	13.1 ± 5.4	-175.5 ± 5.4
inmcm4	63.6 ± 3.7	17.5 ± 5.3	-92.4 ± 5.4
IPSL-CM5A-LR	100.7 ± 3.8	17.7 ± 5.3	-121.2 ± 5.4
MIROC5	147.1 ± 3.7	7.7 ± 5.3	-164.9 ± 5.3
MIROC-ESM	133.4 ± 3.9	16.1 ± 5.5	-151.4 ± 5.3
MPI-ESM-LR	117.6 ± 3.7	12.5 ± 5.3	-138.4 ± 5.4
MRI-CGCM3	116.4 ± 3.8	11.5 ± 5.4	-145.7 ± 5.6
NorESM1-M	164.7 ± 3.7	8.8 ± 5.3	-183.9 ± 5.3
mean ± std. dev.	127.9 ± 27.3	14.4 ± 3.4	-148.5 ± 25.4

TCD
7, 2761–2800, 2013

Table 3. Mean parameters and goodness-of-fit (RMSE) of a function of the form $a + b \cdot \Delta T + c \cdot \Delta T^2 \cdot \frac{\Delta T}{|\Delta T|}$ fitted to the modeled global glacier mass balance when glacier hypsometry is held constant, and ice volume treated as infinite (Fig. 6). Standard deviation between CMIP5 models given as uncertainty.

scenario		a $\left[\frac{\text{mm SLE}}{\text{yr}}\right]$	b $\left[\frac{\text{mm SLE}}{\text{K yr}}\right]$	c $\left[\frac{\text{mm SLE}}{\text{K}^2\text{yr}}\right]$	RMSE $\left[\frac{\text{mm SLE}}{\text{yr}}\right]$
RCP26	global mean ΔT	1.07 ± 0.19	1.41 ± 0.44	0.72 ± 0.72	1.45
	glacier surface area weighted ΔT	1.12 ± 0.16	0.75 ± 0.19	0.19 ± 0.12	0.87
RCP45	global mean ΔT	1.05 ± 0.20	1.51 ± 0.55	0.76 ± 0.39	3.60
	glacier surface area weighted ΔT	1.11 ± 0.19	0.74 ± 0.23	0.21 ± 0.08	1.77
RCP60	global mean ΔT	0.98 ± 0.12	1.18 ± 0.53	0.82 ± 0.47	1.48
	glacier surface area weighted ΔT	1.05 ± 0.10	0.64 ± 0.19	0.24 ± 0.07	0.94
RCP85	global mean ΔT	0.88 ± 0.44	2.01 ± 1.50	0.62 ± 0.48	11.86
	glacier surface area weighted ΔT	0.97 ± 0.49	0.81 ± 0.49	0.23 ± 0.07	5.71

TCD
7, 2761–2800, 2013

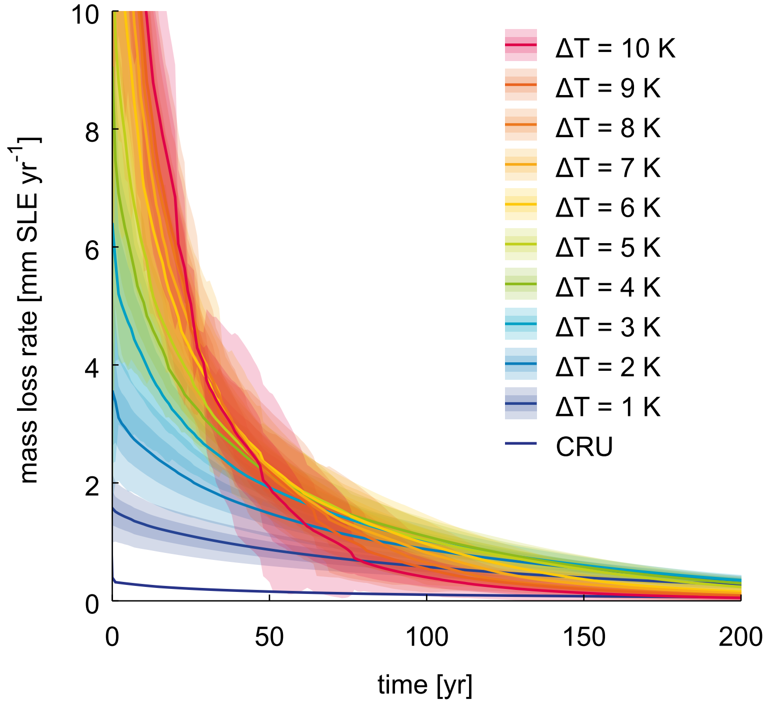

Fig. 1. Rates of global glacier mass loss during the first 200 yr of the equilibrium experiment (Fig. 2). Dark (light) shading indicates one (two) standard deviations. Colors indicate global mean temperature anomaly applied.

TCD
7, 2761–2800, 2013

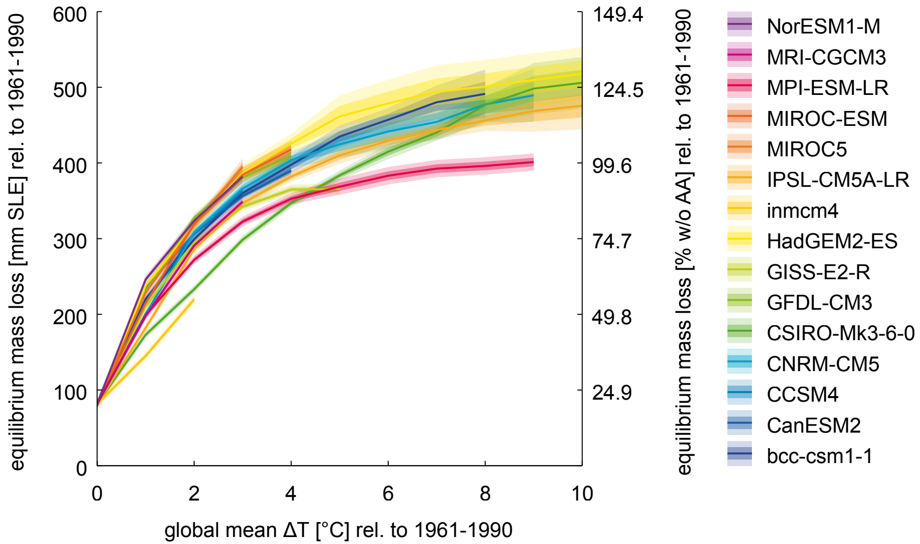

Fig. 2. Equilibrium mass loss of glaciers as a function of global mean temperature anomaly. Dark (light) shading indicates one (two) standard errors. Colors indicate which CMIP5 model was used for forcing. No estimate of the volume of Antarctic peripheral glaciers (AA) is obtained from the model. Therefore, the right axis of (% volume loss) may exceed 100 %.

TCD
7, 2761–2800, 2013

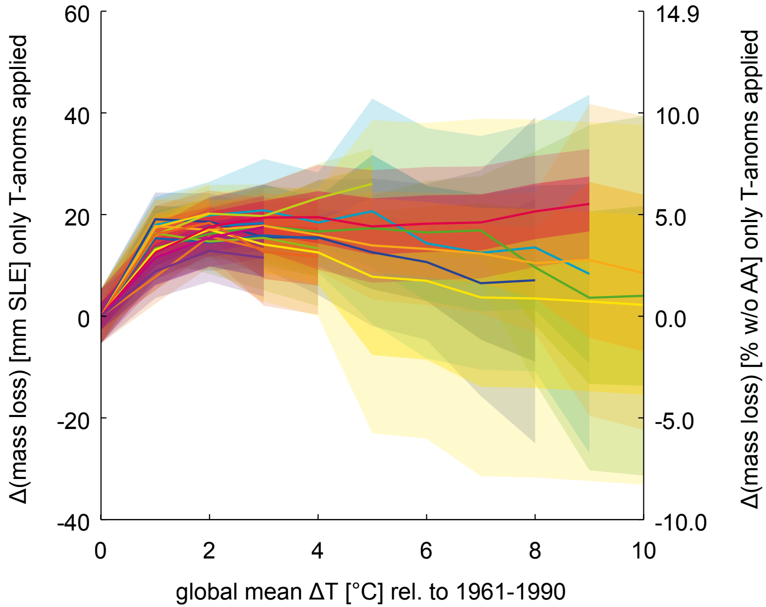

Fig. 3. Additional equilibrium mass loss of glaciers when only temperature anomalies are applied, and precipitation anomalies are ignored. Dark (light) shading indicates one (two) standard errors. Colors as in Fig. 2.

TCD
7, 2761–2800, 2013

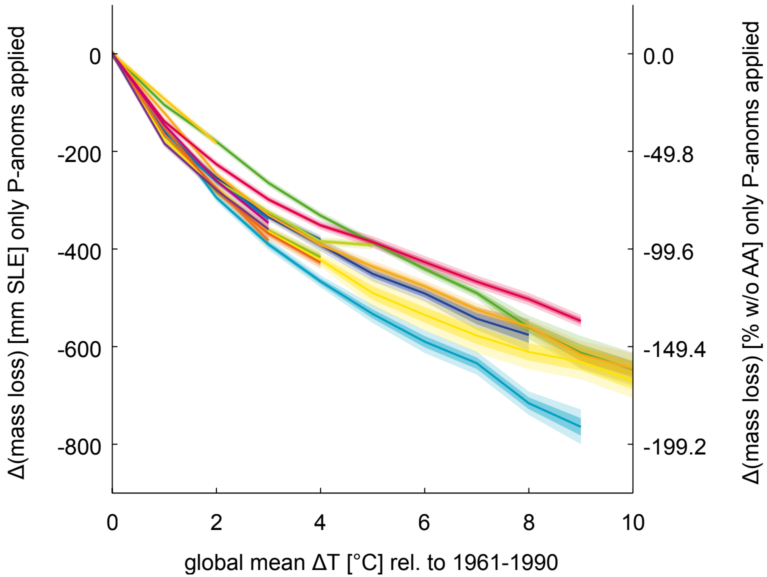

Fig. 4. Additional equilibrium mass loss (negative numbers imply mass gain) of glaciers when only precipitation anomalies are applied, and temperature anomalies are ignored. Dark (light) shading indicates one (two) standard errors. Colors as in Fig. 2.

TCD
7, 2761–2800, 2013

Mechanisms affecting global glacier sensitivity

B. Marzeion et al.

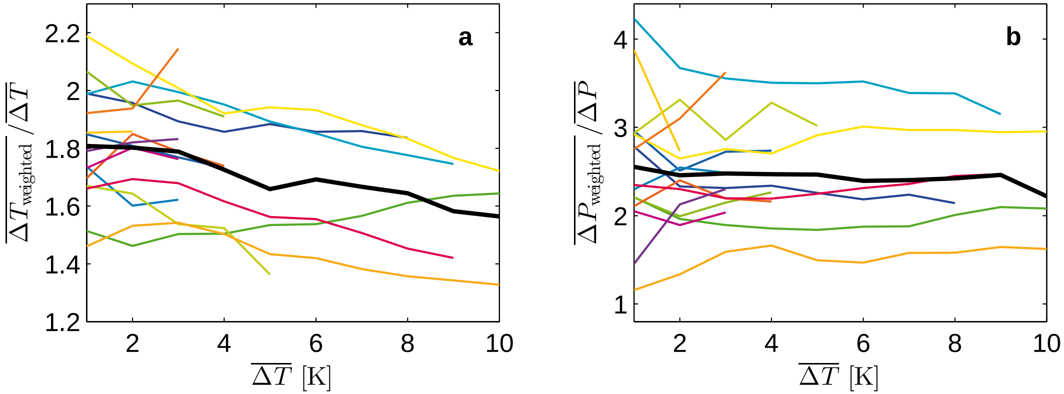

Fig. 5. Temperature and precipitation amplification at the locations of glaciers. **(a)** Amplification of temperature anomalies at the locations of glaciers as a function of global mean temperature anomaly $\overline{\Delta T}$. **(b)** Amplification of relative precipitation anomalies at the locations of glaciers as a function of global mean temperature anomaly $\overline{\Delta T}$. Colors as in Fig. 2.

TCD
7, 2761–2800, 2013

Mechanisms affecting global glacier sensitivity

B. Marzeion et al.

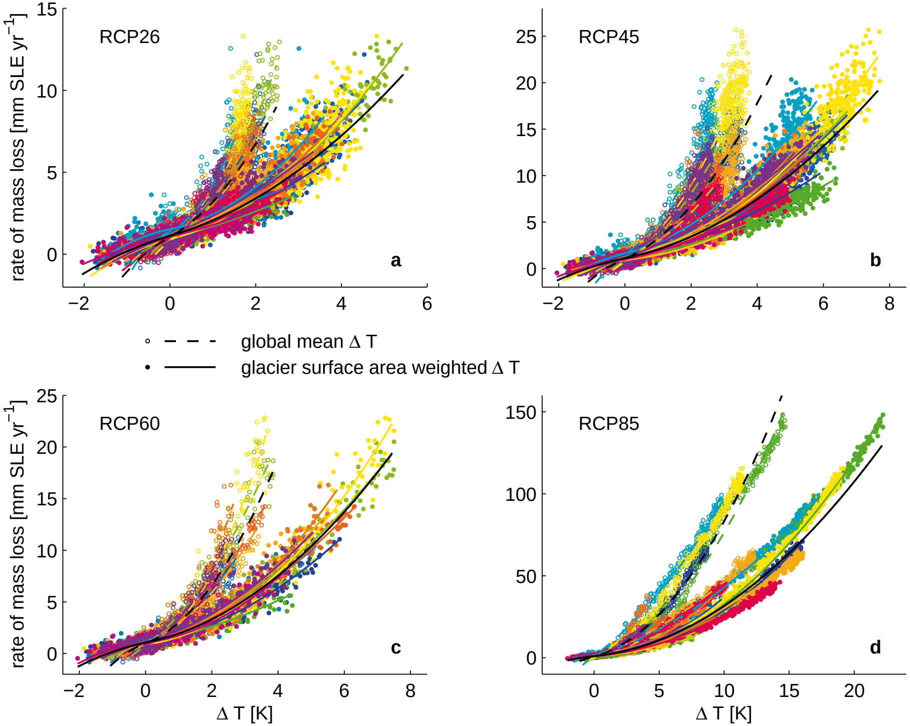

Fig. 6. Global glacier mass balance, expressed in terms of global mean sea level equivalent (SLE), as a function of global mean (open circles, dashed lines) and glacier surface area weighted (filled dots, solid lines) temperature anomalies when glacier hypsometry is held constant, and ice volume treated as infinite. Colored lines show quadratic fits for each individual CMIP5 model, black lines show fits based on mean parameters of colored lines. Colors as in Fig. 2.

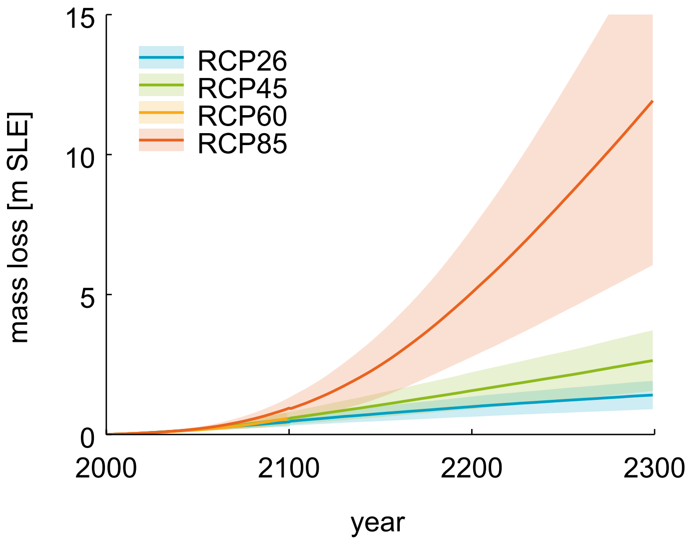

Fig. 7. Global glacier mass loss when glacier hypsometry is held constant, and ice volume treated as infinite. Solid line is ensemble mean, shading indicates ensemble spread (one standard deviation).

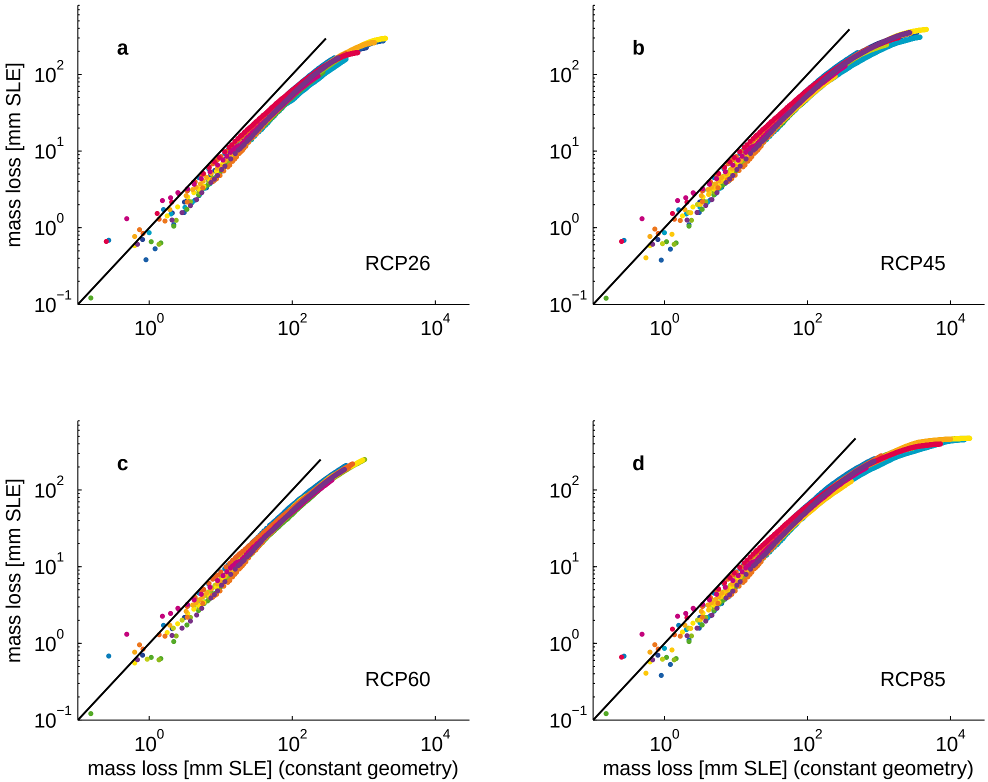

Fig. 8. Global glacier mass loss of Marzeion et al. (2012) versus global glacier mass loss when glacier hypsometry is held constant, and ice volume treated as infinite. Black line is the bisector. Colors as in Fig. 2.

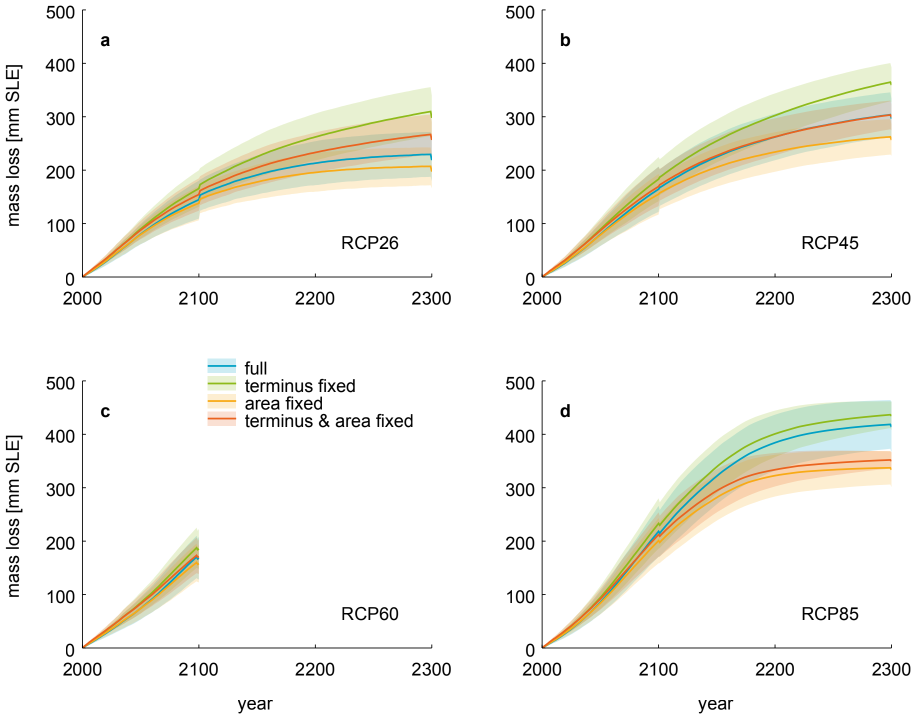

Fig. 9. Effects of different aspects of glacier hypsometry change on glacier mass change; "full" refers to the results of Marzeion et al. (2012) with fully responsive glacier hypsometry. Solid line is ensemble mean, shading indicates ensemble spread (one standard deviation).

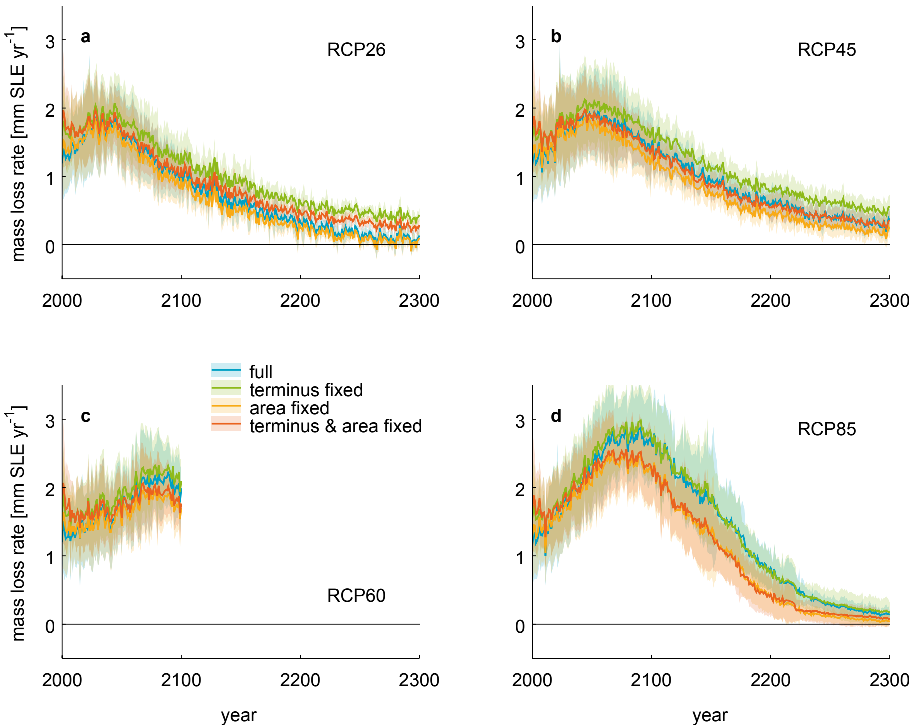

Fig. 10. Effects of different aspects of glacier hypsometry change on glacier mass change rates; "full" refers to the results of Marzeion et al. (2012) with fully responsive glacier hypsometry. Solid line is ensemble mean, shading indicates ensemble spread (one standard deviation).

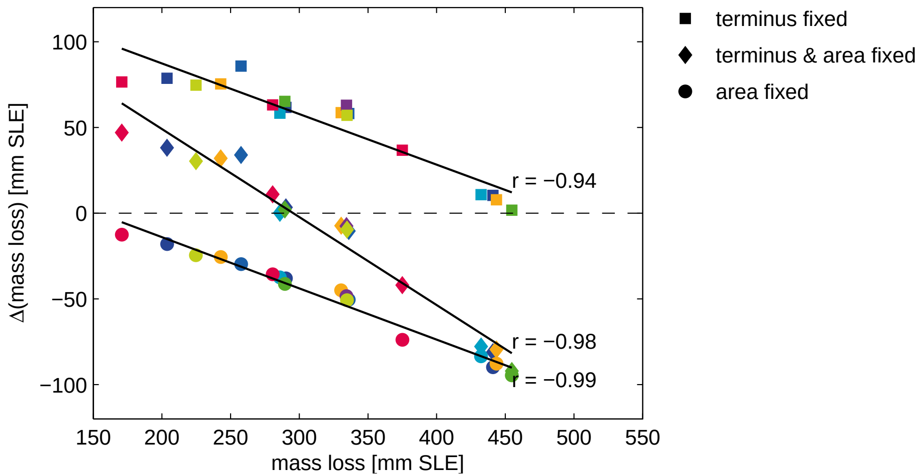

Fig. 11. Summary of the effects of different aspects of glacier hypsometry change on mass loss. Squares: constant terminus elevation, circles: constant surface area, diamonds: constant terminus elevation and surface area. Plotted are the anomalies in the year 2300 as a function of respective mass loss projected in Marzeion et al. (2012) at the same time. Colors as in Fig. 2. No distinction is made between different RCP scenarios.